

# Comparison of Microstructure, Density and Shrinkage Porosity for Casting and Rheocasting of AlSi7Mg alloy

Kawan Abdulrahman ( kawanabdulrahman@gmail.com )

Óbudai Egyetem: Obudai Egyetem

Viktor Gonda Mihály Réger Péter Varga

### Research Article

**Keywords:** Semi-solid forming, Rheocasting, Aluminum alloy AlSi7Mg, Pressure Casting, Metallography, Porosity, Density, Shape factor.

Posted Date: July 13th, 2023

**DOI:** https://doi.org/10.21203/rs.3.rs-3143835/v1

**License:** © ① This work is licensed under a Creative Commons Attribution 4.0 International License.

Read Full License

# Comparison of Microstructure, Density and Shrinkage Porosity for Casting and Rheocasting of AlSi7Mg alloy

Kawan M. Abdulrahman\*\*1, Viktor Gonda2, Mihály Réger3, Péter Varga4

- \*1 Doctoral School on Materials Sciences and Technologies Óbuda University.Budapest, Hungary,
- \*\*I Sulaimani Polytechnic University, Technical College of Engineering, Department of Production Engineering & Metallurgy, Iraq

kawan.abdulrahman@bgk.uni-obuda.hu

- <sup>2</sup>Óbuda University, Bánki Faculty of Mechanical and Safety Engineering.Budapest, Hungary. Budapest, Hungary, gonda.viktor@bgk.uni-obuda.hu
- <sup>3</sup>Óbuda University, Bánki Faculty of Mechanical and Safety Engineering.Budapest, Hungary. Budapest, Hungary, <u>reger.mihaly@bgk.uni-obuda.hu</u>
- <sup>4</sup>Óbuda University, Bánki Faculty of Mechanical and Safety Engineering.Budapest, Hungary. Budapest, Hungary, *varga.peter@bgk.uni-obuda.hu*

#### **Abstract**

With the increasing application of aluminum foundry alloys for automotive and aerospace components, the aluminum industry must pay close attention to component quality and dependability. This article focuses on the interpretation of the relative density and porosity of Al foundry casting and rheocasting alloys AlSi7Mg. The most popular Al-Si alloy grain refinement utilized in the casting and rheocasting processes is AlSi7Mg. The limitations are using comparable density findings to determine the quality of a component of casting or rheocasting state. Two approaches are employed to attain this goal, first the theoretical analysis using the JMatPro software, which offers density distribution results depending on the chemical composition of the aluminum alloy. Second, the experimental Archimedes method, which provides density data on actual aluminum castings alloy. This study advances substantial research on microstructure, grain sizes, form shape factors, theoretical and practical density, shrinkage porosity, casting and rheocasting application samples alloy, and potential industrial applications of AlSi7Mg. The results show that the average grain size is significantly more uniform in the rheocasting comparing to casting average grain size results. In addition, the results from the metallographic image analysis of casting and rheocasting application shows five different zones from the bottom to the top of the sample. Finally, the study observed that the shrinkage porosity in the casting application sample is higher than those of rheocasting application sample.

#### Keywords

Semi-solid forming, Rheocasting, Aluminum alloy AlSi7Mg, Pressure Casting, Metallography, Porosity, Density, Shape factor.

#### 1 Introduction

The casting components have a complete filling at low solid fractions, according to the results. Microstructure size, and solid fraction management for micro shrinkage level are essential. Therefore, this works continues to find further potential commercial applications in gravity die casting [1,20]. Rheocasting alloys used in the telecommunications industry like a hollow filter with a thin wall thickness (about 0.35 mm) [29]. Current aluminum vehicle parts, such as wheels, engines, and transmission components are produced utilizing the tilting rheocasting semi-solid process to decrease gas porosity. By focusing on alloy modification and casting process parameters [25,26], evaluations of slurry quality manufactured utilizing cast procedures, as well as the final microstructure and qualities of rheocasting components [27,29]. They have produced very positive results in both castability and final properties.

The casting aluminum alloy  $AlSi_7Mg$  is to identify the key few processing factors that are critical in the emergence of the shrinkage porosity and to choose remedial actions to reduce the fault so that the components passed a leak test [2,4].

Thanabumrungkul et. al., (2019) found that the casting, parts have complete filling at low solid fractions and the casting yield is also higher than conventional gravity sand casting. Cycle durations, microstructure size, homogeneity, and solid fraction control for micro shrinkage level were the key factors imposed on gravity die casting. Slurry gravity die cast components experience less micro shrinkage than liquid cast components [3,20]. The microstructure and porosity persangage along the components support the findings. Thanabumrungkul et. al., (2019) found that the optimizing the solid fraction and mold temperature

management are required to reduce shrinkage porosity. Also, shrinkage porosity, microstructure size, and homogeneity continue to squander production resources [20].

The rheo-diecastings' microstructure and solidification flaws could be effectively improved by the semi-solid slurry. The mechanical properties of the rheo-diecastings are superior to those of the typical die castings because a high number of the tiny size primary -Al grains with uniform distribution are involved in their deformation. [28,31]

In a tilting pour permanent mold, the main phase -cu was surrounded by a sharp angle that was lessened with increased heat treatment stpes, better semi-solid microstructure shape, and decreased liquid droplets with improving grain sizes, form shape factors, density, shrinkage porosity properties of semi-solid copper Alloy [4,5,6,20]. For Al-Si alloy grain refining, AlSi<sub>7</sub>Mg is the most widely used throughout the casting and rheocasting processes [7,8].

Research on microstructure, grain sizes, form shape factors, theoretical and actual density, shrinkage porosity, casting and rheocasting application samples alloy, and possible industrial applications is significantly advanced by this work. The paper shows that a relative density result derived from Archimedes' measurements must be accompanied by a description of the theoretical density. The shrinkage porosity in the casting application sample is larger than that of the rheocasting application sample parts. Porosity, which is generated mainly by solidification shrinkage and the development of dissolved gases, is one of the most severe issues in aluminum castings. Although porosity is unavoidable in each casting, it may be highly damaging to the mechanical characteristics.

#### 2 Experimental procedures

#### 2.1 Material

The material used in the investigations was the aluminum alloy AlSi7Mg (EN AB-42000). The chemical composition is shown in Table 1.

Table 1. The chemical composition of AlSi7Mg alloy in wt%

Al	Mg	Si	Sn	Fe	Mn	Cu	Ti	Zn	Pb	Ni
Bal.	0.25-	6.5-7.5	0.05	0.45	0.35	0.15	0.05-	0.15	0.15	0.15
	0.65						0.20			

Al-Si alloys are refined chemically using traditional techniques [6,30]. The aluminum alloy AlSi<sub>7</sub>Mg is an alloy in the wrought Al-Si series 4xxx. It is generally processed by rolling and extrusion [9,10]. Despite its uncommon practice with this alloy, it can also be forged and cladded. The main applications are scaffolding elements, rail coach parts, offshore constructions, containers, machine-building, and mobile cranes. The use of alloy AlSi<sub>7</sub>Mg in the above applications displays good resistance to dynamic loading conditions. This is attributed to its fine-grained structure [10,11]. This grade is commonly used for pressure-tight castings that are susceptible to fatigue loading [8, 9]. After heat treatment, it has good corrosion resistance and high strength. Further, this alloy is excellent for marine applications [12].

In the practical alloy  $AlSi_7Mg$ , aluminum alloys contents of Si~6.5-7.5 wt%, generally by Si~of more than one and semi-solid temperature [2,13,14].

#### 2.2 Processing

The two types of aluminum casting alloys are explained, and examples from pressure casting and rheocasting processes are contrasted.

# 2.2.1 Pressure casting

A pressure chamber and compressor are used in the pressure casting process to remove air bubbles from a casting resin or mold rubber. It is the most effective technique for guaranteeing bubble-free castings [28]. Professional prototype model makers who cannot tolerate even one bubble frequently utilize the pressure casting technique. Casting will be rejected if there is even one bubble on its surface [5,15].

#### 2.2.2 Semi-solid rheocasting

Rheocasting is one of the semi-solid metals (SSM) processing methods; it is carried out with the casting and rheocasting of semi-solid alloys, producing non-dendritic microstructure and solid spheroids [16, 17]. The rheocasting procedure for producing slurries of the alloys as mentioned above is thoroughly discussed in [5,10].

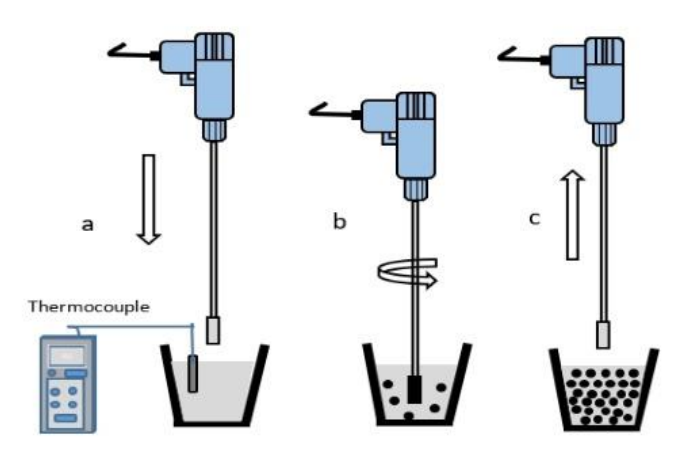


**Figure 1.** Rheocasting process steps: (a) a solid block of the same alloy, fastened to a stainless-steel rod in advance, (b) dissolved in the melt with synchronous stirring action, and (c) the resulting slurry.

The raw material for semi-solid rheocasting (SSR) is obtained directly from ingot operations, with no intermediary solidification phase [17, 18]. The molten metal is poured into a steel mold at a little over liquidus temperature and then treated to produce a globular microstructure using the rheocasting process [19,20]. This test necessitates the use of a steel mold. The molten metal is kept above the solidus temperature at an alloy's semi-solid temperature. Stirring is applied for some time. The semi-solid state interacts with the liquid-solid alloy as the steel rod rotates, and a temperature gradient between the melt and the rod is shown in (Figure 1) [16]. As a result, the melt partially solidifies on the rod's surface [16, 17].

#### 2.3 Application sample

The Casting and Rheocasting application samples are shown in (Figure 2).



Figure 2. Casting and rheocasting application samples.

Area position one was obtained from the lowest samples, just below the sprue; area position two was taken from the center; and area position three was taken from the bottom of the alloy, as illustrated in (Figure 3). The samples for area position four were evaluated horizontally between area positions three and five, with area position five being obtained from the top samples.

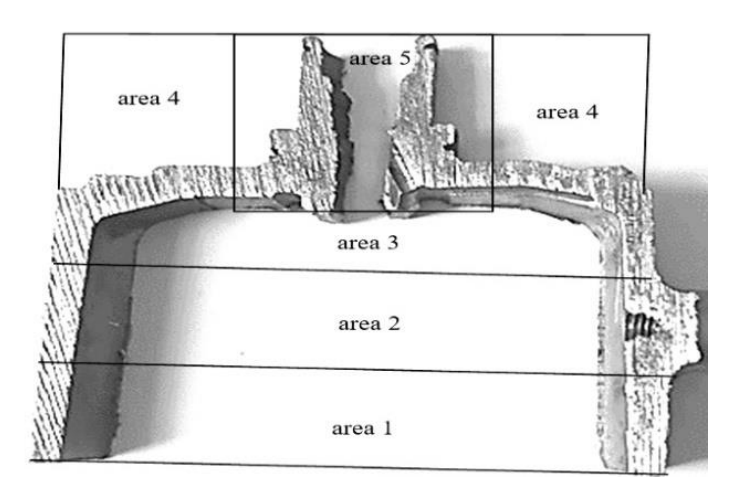


**Figure 3.** Five area positions of the analyses.

#### 2.4 Analysis of Microstructure

Optical microscopy (Neophot 2) was used to investigate the microstructure of the materials. All Samples were cut, mounted, grind, polished, and etched by Keller solutions.

The linear intercept analysis approach was used to determine the average grain size.

#### 3 Results and discussion

#### 3.1 Alloy properties

Data such as temperature versus solid percentage and liquidus and solidus temperatures were computed to evaluate the solidification properties within the investigation's compositional range, as shown in (Figure 4).

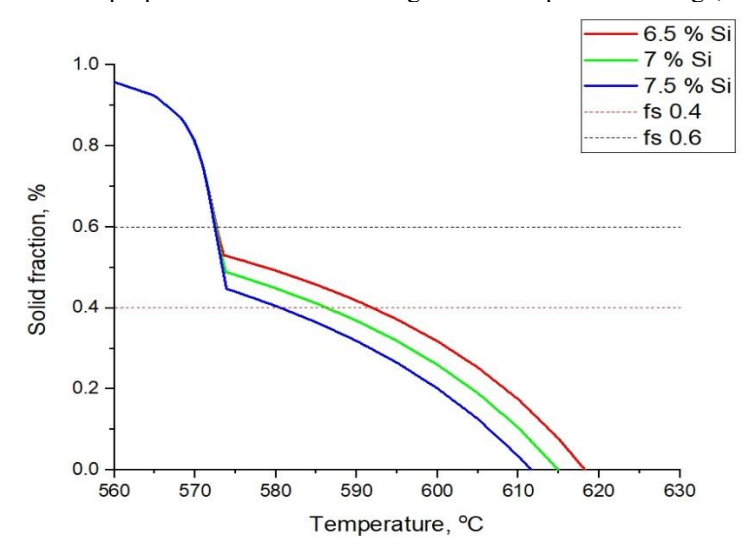
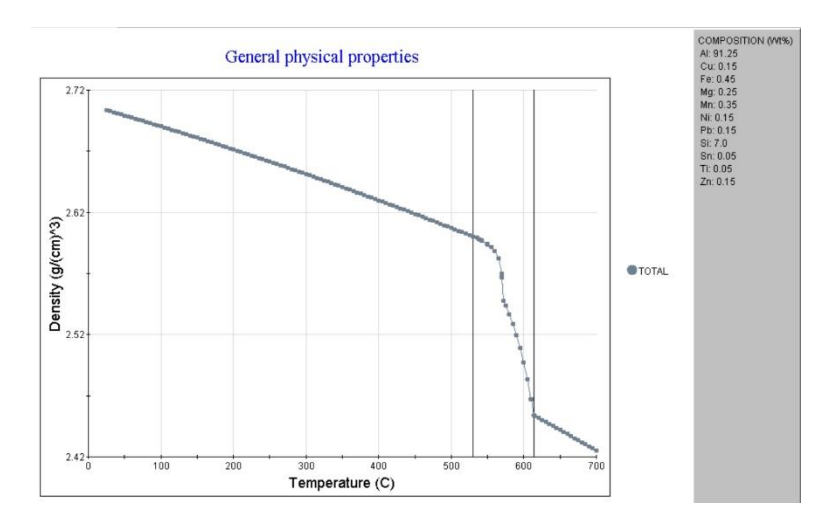


Figure 4. The solid fraction, liquids, and solidus temperature of ALSI7MGalloy with different Si content.

The sensitivity of the solid fraction and solidification range, which are essential parameters for the usability of a semi-solid method for alloys with varied Si concentrations, were assessed using thermodynamic estimations [21, 22]. The slope of the solid fraction vs temperature curve is described as temperature sensitivity, which is written as df/dT [23]. The solid fraction has a high-temperature sensitivity, which indicates that a slight temperature change generates a huge change in the solid fraction, making it difficult to control the solid—liquid melt and get the required microstructure [24].

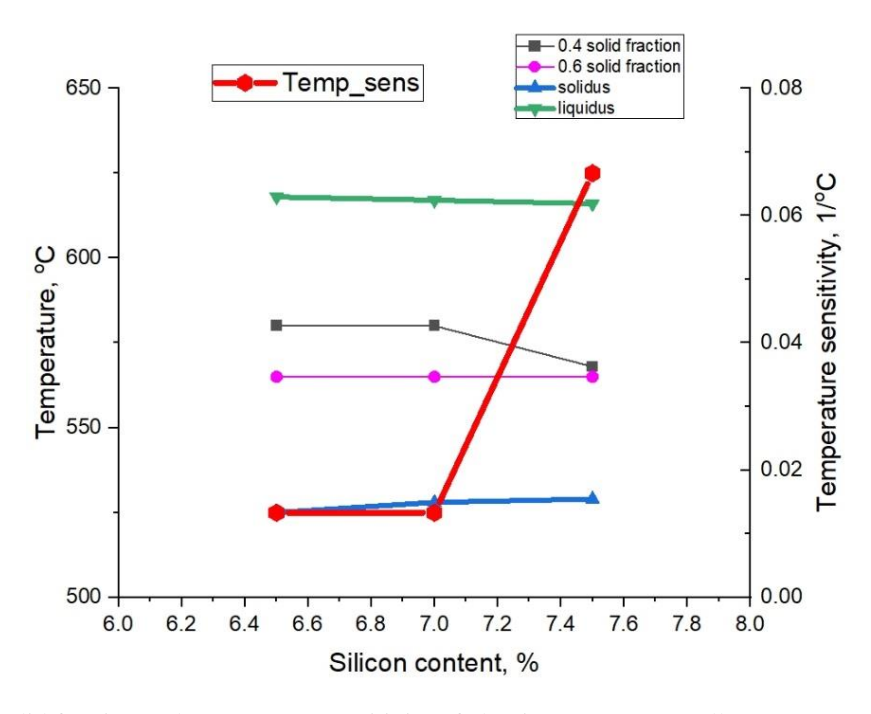
The theoretical density data of the casting alloy is 2.7 g/cm<sup>3</sup> depending on the alloy's chemical compositions, which is shown in (Figure 5). Additional calculations using the JMatPro software showed that the eutectic point of the alloy with the highest alloying content occurred when 2.7 g/cm<sup>3</sup> of the density had formed; for the practical density in Archimedes method, 2.64 g/cm<sup>3</sup> of the solid density had been found.



**Figure 5.** Theoretical Density of Aluminum EN AB-42000 alloy by using JMatPro.

#### 3.2 Controlling the solid fraction and mold temperature

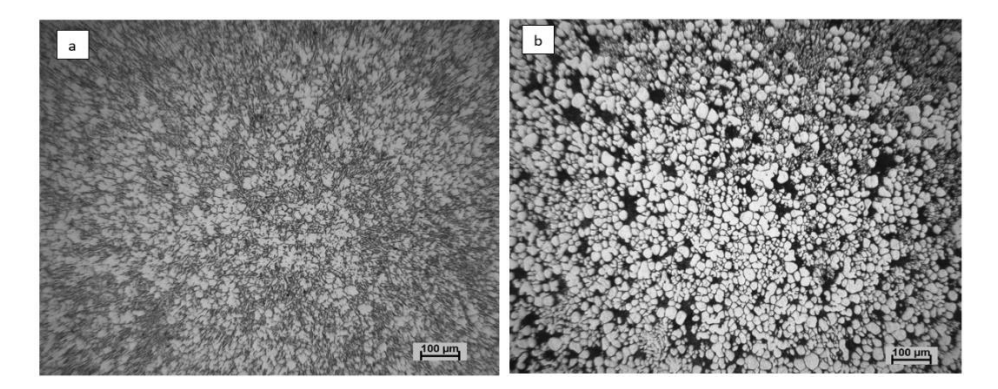
With varied Si concentrations, (Figure 6) illustrates the solid fraction of the alloys as a function of temperature. The liquidus temperature drops as the Si concentration rises, whereas the eutectic temperature rises. With variable Si concentration, Due to variations in the latent heat that occurs during the solidification of the alloy, the temperature sensitivity of the solid fraction decreases as the solid fraction rises to 0.6. The eutectic reaction occurs at a solid fraction of 0.6, significantly increasing temperature sensitivity as a function of solid fraction. A greater Si concentration in the solid fraction results in reduced temperature sensitivity before the eutectic reaction commences. The decreased sensitivity may be due to the increased Si content creating small amounts of the  $\alpha$ -Al phase, releasing small amounts of latent heat during solidification. Furthermore, the peaks of the curves grow as the Si concentration increases, indicating a high quantity of liquid phase in the eutectic process.



**Figure 6.** Solid fraction and temperature sensitivity of aluminum ALSI7MGalloy.

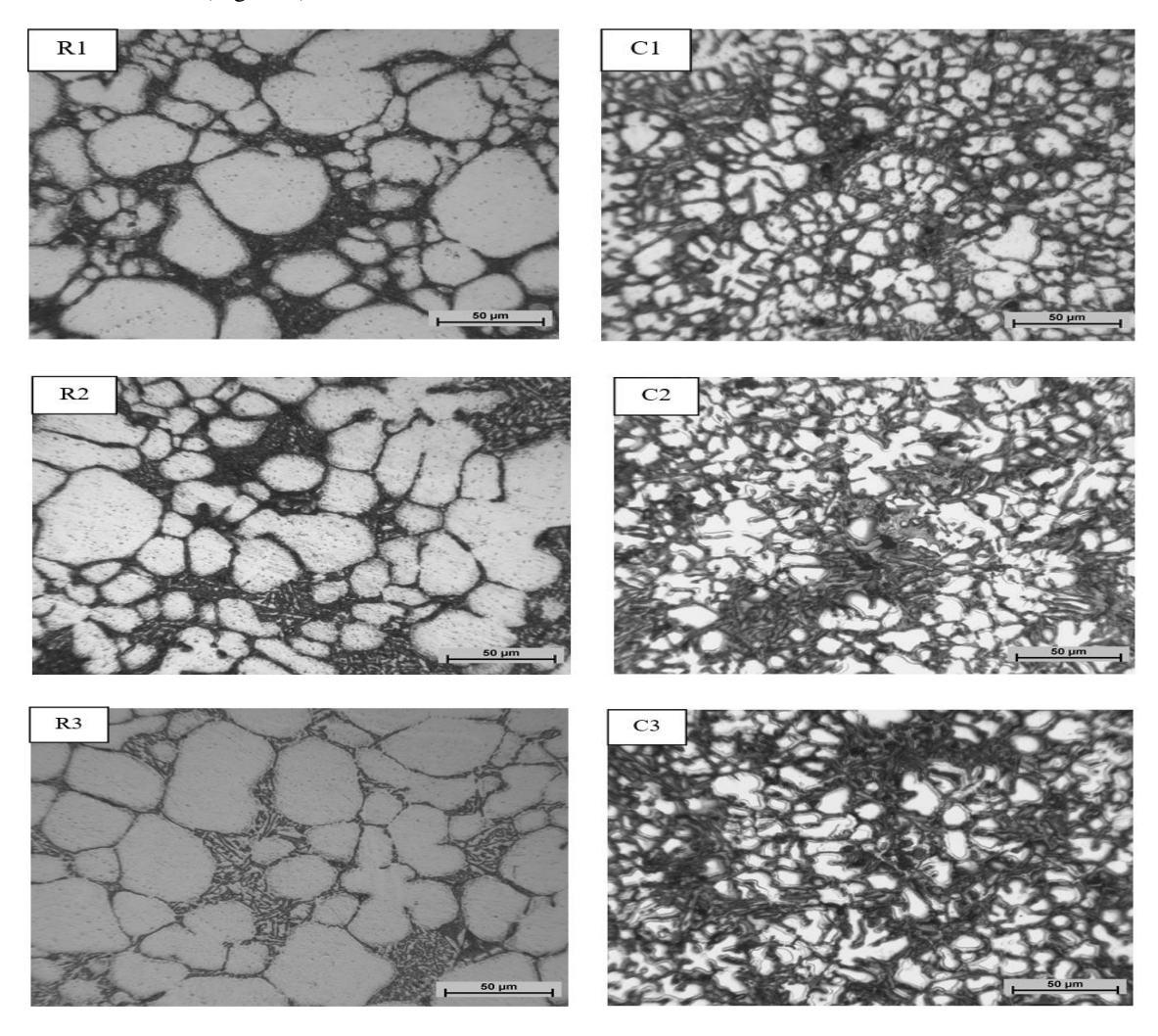
#### 3.3 Microstructure

At the alloy's semi-solid temperature, the nuclei are generated and then flung into the melt by the rotating motion of the rod, resulting in a globular microstructure of tiny grains. shown, the fine dendritic structure of the casting alloy is shown in (Figure 7a), while the microstructure of the rheocast sample is shown in (Figure 7b).



**Figure 7.** The microstructure of Casting (a) and Rheocasting (b) application samples.

In the rheocasting alloy, the average grain size was substantially more uniform. The example of the microstructure at location R5 in (Figure 8) shows this as well.



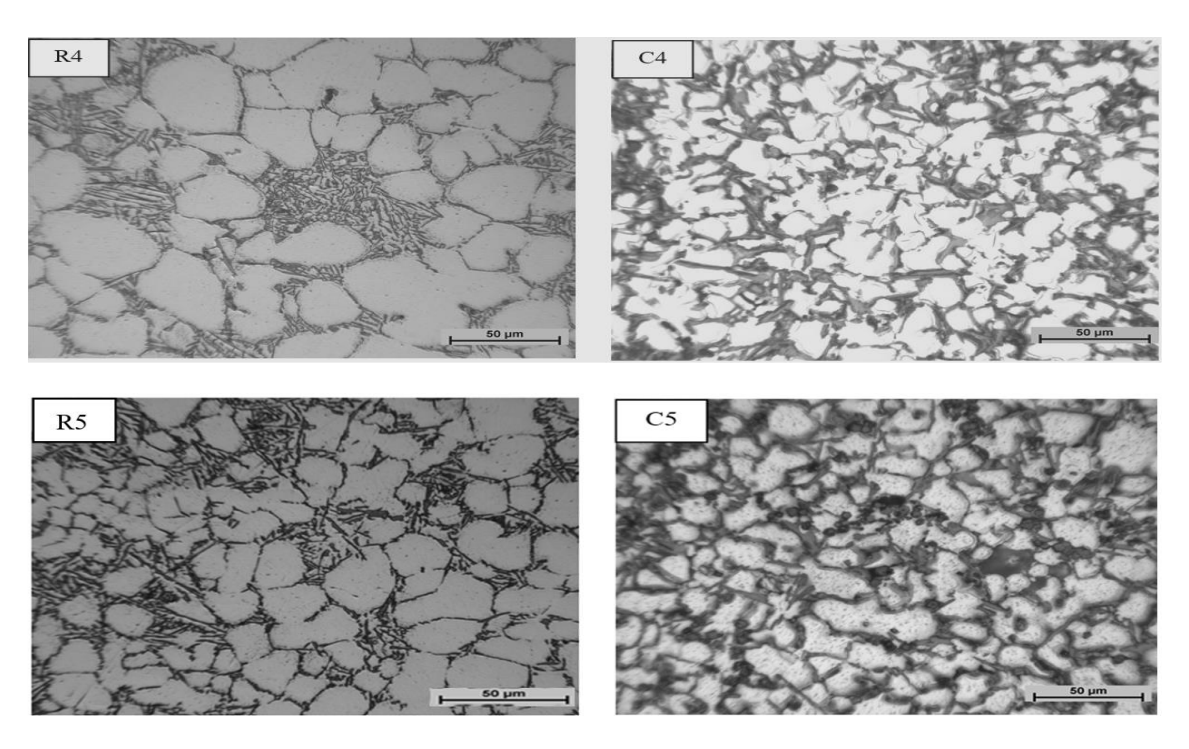
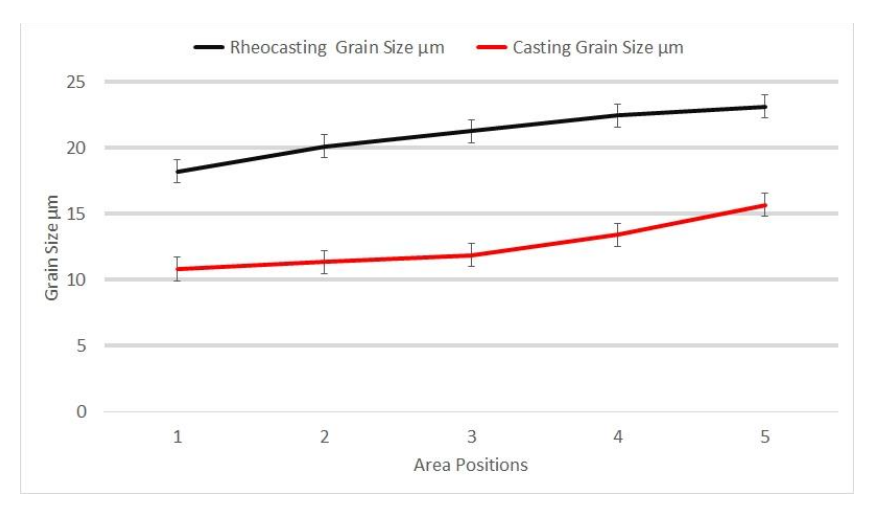


Figure 8. The microstructures of casting (C) and rheocasting (R) application samples.

The microstructure of the five locations is shown in (Figure 8): bottom (Position R1, C1) near the sprue, higher (Position R2, C2), middle (Position R3, C3), near-bottom (Position R4, C4), and top (Position R5, C5) (Position R5, C5). The (R) depicts a rheocasting microstructure with a fine spherical shape phase structure along the sample part, whereas Figure (C1) shows a small dendritic phase structure along the sample part, and the (C) depicts a casting microstructure with a sizeable dendritic phase structure along the sample part.

#### 3.4 Grain size

The macrostructure comparison between casting and rheocasting application samples is shown in (Figure 9). The results reveal that rheocasting provides a more homogenous macrostructure than casting. In microstructure analysis, the results also confirm the main grain size distribution. At the first area positions, the significant grain sizes of casting and rheocasting are  $10.821\,\mu m$ , and  $18.21\,\mu m$ , while at the second area positions the corresponding values are  $11.34\,\mu m$ , and  $20.122\,\mu m$ , respectively. At the third and fourth area positions, the primary grain sizes of casting and rheocasting are  $11.88\,\mu m$ ,  $21.76\,\mu m$ ,  $12.40\,\mu m$ , and  $21.87\,\mu m$ , respectively. At the fifth area locations, the primary grain sizes of casting and rheocasting are  $16.67\,\mu m$  and  $23.13\,\mu m$ , respectively.



**Figure 9.** The primary  $\alpha$  grain size of the casting and rheocasting application samples.

#### 3.5 Shape factor

The shape factor of casting and rheocasting application examples is shown in (Figure 10). The shape factor of semi-solid rheocasting area samples is significantly larger than the shape factor of casting.

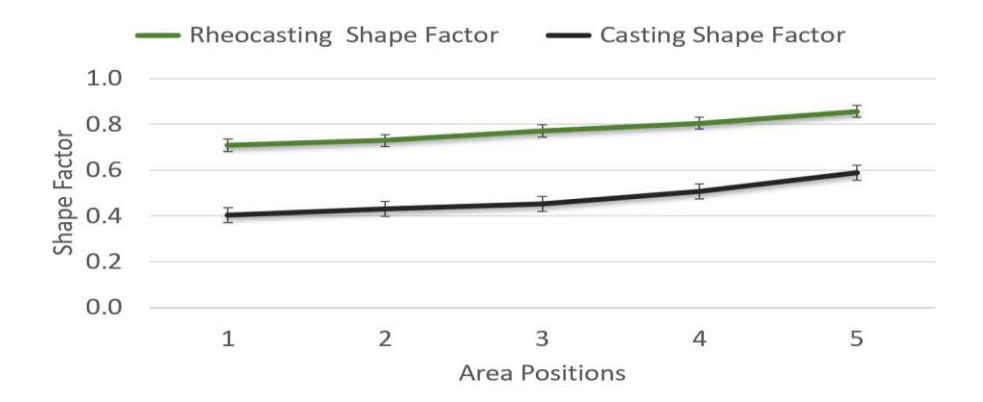


**Figure 10.** The shape factor of casting and rheocasting application samples.

The shape factor values in both alloys were increased from the down to the top positions. The structure with the smallest grain size showed the highest performance in semi-solid creation and the best mechanical characteristics and microstructure properties; the shape factors above 0.6-0.7 had the most homogenous properties aside from the primary phases' globular size. A spherical particle was assigned a value of 1 in this technique [18]. The shape factor and mold temperature control must be fine-tuned [19].

#### 3.6 Density and porosity

The Archimedes approach offers access to global data, allowing the estimation of the relative density of a part based on its volume. The Archimedes method has limitations since it must choose which reference material to use as a basis for predicting relative density. For example, in our examination of two aluminum alloys, we discovered that picking a material equivalent to the foundry alloy, despite being historically used as a reference in the literature, can result in more than 100% relative densities. Furthermore, the findings demonstrate that the Archimedes technique produces accurate results, particularly when selecting reference materials for theoretical computing density. For example, depending on the testing conditions, the density of the casting alloy was lower than that of the rheocasting alloy.

Calculate the mass and volume of the aluminum alloys using the Archimedes method. Calculate the density of aluminum alloys by determining the mass and volume of two alloys using Archimedes' Principle and determine the percent difference between your calculated densities in casting alloy and rheocasting alloy.

The practical density data of the casting alloy and rheocasting sample were 2.64 g/cm<sup>3</sup> and 2.69 g/cm<sup>3</sup>; the results are shown in (Figures 11 and 13).

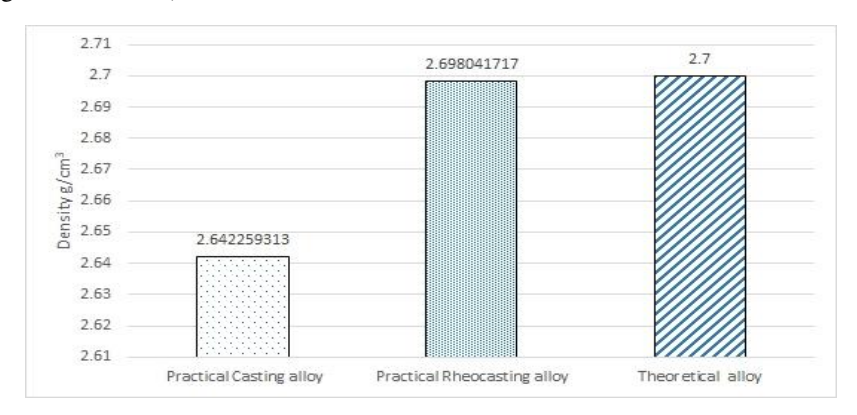
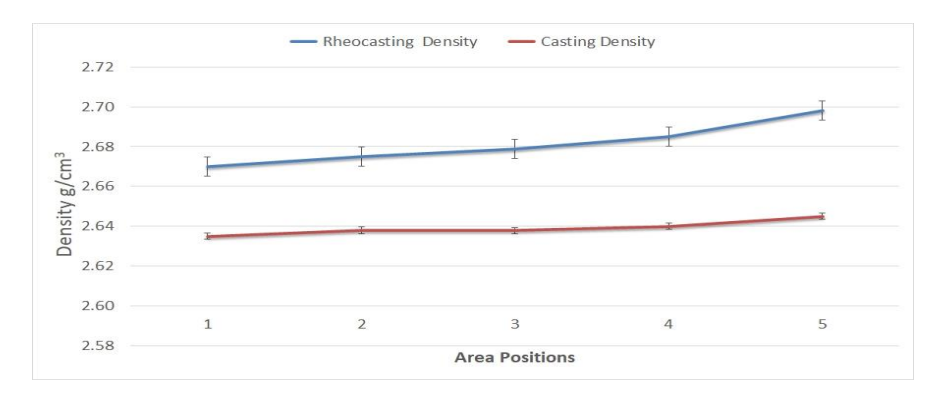


Figure 11. Density values of the cast, the rheocast alloys, and the theoretical density.

The density of the five-area positions of casting and rheocasting application samples is shown in (Figure 12). The shape density in both alloys was increased from the down to top positions.



**Figure 12.** Density values of five-area positions the cast, the rheocast alloy.

The shrinkage porosity data of the casting alloy and rheocasting sample were 2.14% and 0.07%. The results are shown in (Figure 13). However, less micro shrinkage porosity occurs when the rheocasting time is extended. The results demonstrate that the rheocasting sample has reduced micro shrinkage, which can be handled by optimizing the solid percentage and controlling the mold temperature. Porosity, considered one of the most essential elements of quality, has long been blamed for poor mechanical qualities.

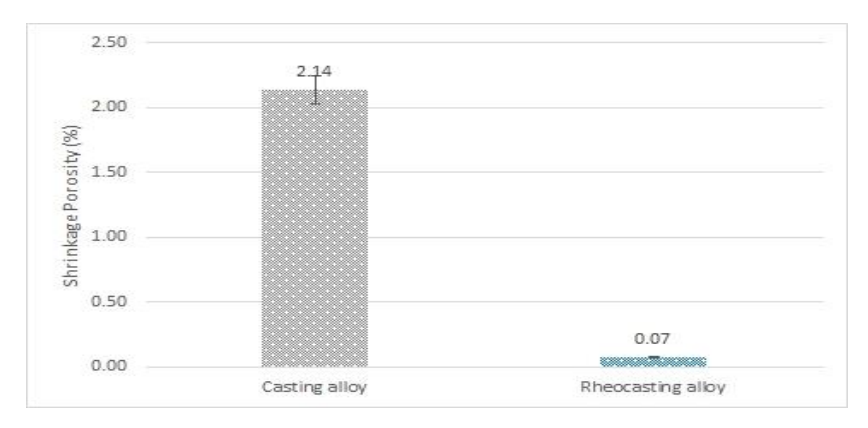


**Figure 13.** Shrinkage porosity values of individual casting and rheocasting alloy.

The shrinkage porosity data of the casting alloy and rheocasting sample were 2.14% and 0.07%. The results are shown in (Figure 13). However, less micro shrinkage porosity occurs when the rheocasting time is extended. The results demonstrate that the rheocasting sample has reduced micro shrinkage, which can be handled by optimizing the solid percentage and controlling the mold temperature. Porosity, considered one of the most essential elements of quality, has long been blamed for poor mechanical qualities.

In observing the micro-porosity volume of the casting alloy of the five-area sample from near the top casting work, significantly different big and small micro-porosity was found as shown in (Figures 14a and 14b).

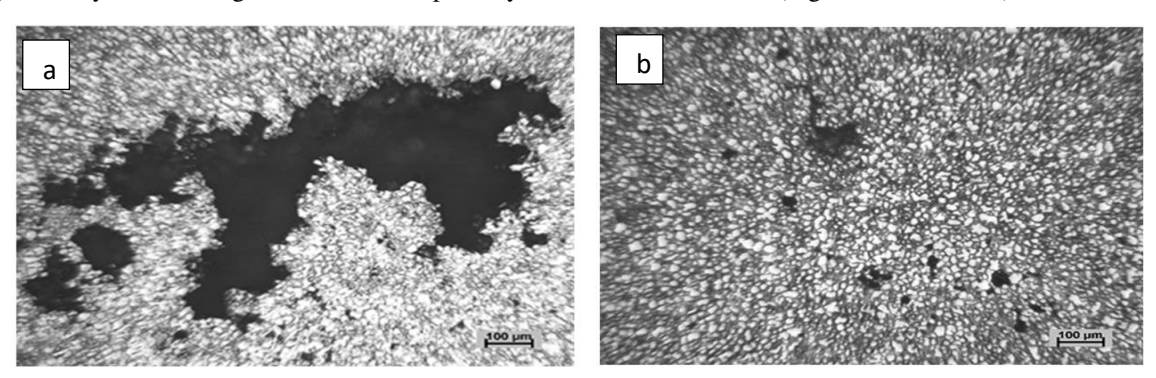
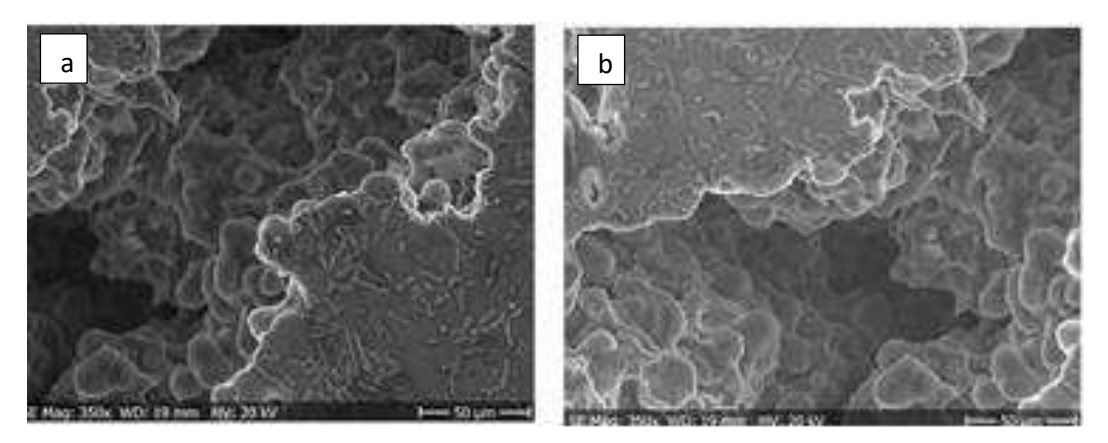


Figure 14. big and small micro-porosity volume in five areas casting alloy sample.

The big and small porosity volume of aluminum ALSI7MGalloy was monitored via a scanning electron microscope. The result of (Figure 15) shows the two-area micro porosity volume in the casting alloy sample. (Figure 15 a and b) show two types of micro-porosity volume large and small. This outcome validates the low casting density and shrinkage porosity results.



**Figure 15.** The structure of the porous material of AlSi7 alloy: (a) Large Micro Porosity volume; (b) small micro-Porosity volume scanning electron microscope image (JSM 5310, SEM H<sub>V</sub> 20.0 k<sub>V</sub>) in two areas casting alloy sample.

#### 4 Conclusions

The study concludes with an analysis of the metallographic images to calculate the primary  $\alpha$  grain size of casting and rheocasting application in five different zones and the sample from the bottom to the top of the casting. In addition, the results show that the  $\alpha$  average grain size and shape factor was significantly more uniform in the rheocasting comparing casting average grain size results. The following conclusions are drawn:

- Micro shrinkage in the rheocasting application is lower than in the casting application sample. The
  microstructure and porosity percentage along the rheocasting application components support the
  findings.
- The average primary grain sizes of rheocasting application sample parts are less than casting
  application sample parts. The microstructure homogeneity of the rheocasting application is also
  improved.
- The metallographic image applications in five different zones from the bottom to the top have significantly more uniformity in the rheocasting comparing casting average grain size results.
- The shrinkage porosity in the casting application sample is higher than those of rheocasting application sample parts, microstructure, and Scanning Electron Microscope images along the parts confirm the results.
- The shape factor arrangement is a factor to reduce shrinkage porosity. The solid fraction and temperature sensitivity management must be tuned to reduce shrinkage porosity.

#### **Funding**

The authors declare that no funds, grants, or other support were received during the preparation of this manuscript.

## **Competing Interests**

The authors have no relevant financial or non-financial interests to disclose.

#### **Author Contributions**

All authors contributed to the study conception and design. Material preparation, data collection and analysis were performed by Kawan M. Abdulrahman, Viktor Gonda and Mihály Réger. The first draft of the manuscript was written by Kawan M. Abdulrahman and all authors commented on previous versions of the manuscript. All authors read and approved the final manuscript.

#### References

- [1] Pola, Annalisa, Marialaura Tocci, and Plato Kapranos. (2019), Microstructure and properties of semisolid aluminum alloys: a literature review, Metals 8, no. 3 (2018): 181.
- [2] de Terris, Thibaut, O. Andreau, P. Peyre, F. Adamski, I. Koutiri, C. Gorny, C. Dupuy, Optimization and comparison of porosity rate measurement methods of Selective Laser Melted metallic parts, Additive Manufacturing 28.
- [3] Maskery, Ian, N. T. Aboulkhar, M. R. Corfield, Christopher Tuck, A. T. Clare, Richard K. Leach, Ricky D. Wildman, I. A. Ashcroft, Richard JM Hague, (2016), Quantification and characterisation of porosity in selectively laser melted Al–Si10–Mg using X-ray computed tomography, Materials Characterization 111.
- [4] Gunasegaram, D. R., D. J. Farnsworth, and T. T. Nguyen, Identification of critical factors affecting shrinkage porosity in permanent mold casting using numerical simulations based on design of experiments, Journal of materials processing technology 209, no. 3, (2009)
- [5] Janudom, S., T. Rattanochaikul, R. Burapa, S. Wisutmethangoon, and J. Wannasin. (2010), Feasibility of semi-solid die casting of ADC12 aluminum alloy." Transactions of Nonferrous Metals Society of China 20, no. 9, 1756-1762.
- [6] Arvieu, Corinne, C. Galy, E.Le Guen, E. Lacoste, (2020), Relative density of SLM-produced aluminum alloy parts: Interpretation of results, Journal of Manufacturing and Materials Processing 4, no. 3.
- [7] Pezda, J, (2009), Effect of modifying process on mechanical properties of EN AB-42000 silumin cast into sand moulds, Archives of Foundry Engineering 9, no. 4.
- [8] Pezda, J., (2011), Effect of T6 heat treatment on mechanical properties and microstructure of EN AB-42000 alloy modified with strontium, Archives of Foundry Engineering 11.
- [9] Blad, Madeleine, B. Johannesson, P. Nordberg, Johannes Winklhofer, (2016), Manufacturing and fatigue verification of two different components made by semi-solid processing of aluminium TX630 alloy, In Solid State Phenomena, vol. 256, pp. 328-333.
- [10] Pezda, J., (2014), Influence of heat treatment parameters on the mechanical properties of hypoeutectic Al-Si-Mg alloy, Metalurgija 53, no. 2.
- [11] Pezda, J., (2012), T6 Heat Treatment of Hypo-eutectic Silumins in Aspect of Improvement of Rm Tensile Strength, Archives of Foundry Engineering 12, no. 2s.
- [12] Arrabal, R., B. Mingo, A. Pardo, M. Mohedano, E. Matykina, I. Rodríguez, (2013), Pitting corrosion of rheocast A356 aluminium alloy in 3.5 wt.% NaCl solution, Corrosion Science 73,
- [13] De Mori, Alessandro, G. Timelli, F. Berto, A. Fabrizi, (2020), High temperature fatigue of heat treated secondary AlSi7Cu3Mg alloys, International Journal of Fatigue 138.
- [14] Blad, Madeleine, B. Johannesson, P. Nordberg, J. Winklhofer, (2016), Manufacturing and fatigue verification of two different components made by semi-solid processing of aluminium TX630 alloy, In Solid State Phenomena, vol. 256, pp. 328-333.
- [15] Vijayaram, T. Raghavan, (2012), Counter Pressure Casting Technique for Aluminium Foundries, Metal world 12.
- [16] Bonollo, F., J. Urban, B. Bonatto, M. Botter, (2005), Gravity and low pressure die casting of aluminium alloys: a technical and economical benchmark, la metallurgia italiana.
- [17] Pola, Annalisa, M. Tocci, P. Kapranos, (2018), Microstructure and properties of semi-solid aluminum alloys: a literature review, Metals 8, no. 3.
- [18] Kirkwood, David H., M. Suéry, P. Kapranos, Helen V. Atkinson, Kenneth P. Young, (2010), Semisolid processing of alloys. Vol. 124.
- [19] Zhang, Ying, Qiang Ma, S. Sheng Xie, M. Peng Geng, J. Hua Xu, Hong Min Guo, H. Bo Zhao, (2011), Investigation in Rheocasting-rolling for Semi-solid Magnesium Alloy Used by Slope, In Advanced Materials Research, vol. 146, pp. 1561-1564
- [20] Thanabumrungkul, S., W. Jumpol, R. Canyook, N. Meemongkol, Jessada Wannasin, (2019), Characterization of Microstructure and Shrinkage Porosity of a Semi-Solid Metal Slurry in Gravity Die Casting, In Solid State Phenomena, vol. 285, pp. 161-166.
- [21] Kang, B. Keun, Il Sohn, (2019), Effects of Si Content and Forging Pressure on the Microstructural and Mechanical Characteristics in Semi-solid Forging of Al-Si-Mg Alloys, Metallurgical and Materials Transactions A 50.
- [22] Zhang, Duyao, H. V. Atkinson, H. Dong, Q. Zhu, (2017), Differential scanning calorimetry (DSC) and thermodynamic prediction of liquid fraction vs temperature for two high-performance alloys for semi-solid processing (Al-Si-Cu-Mg (319s) and Al-Cu-Ag (201)), Metallurgical and Materials Transactions A 48.

- [23] Choi, Byoung-Hee, Y. Jang, Byung-Keun Kang, Chun-Pyo Hong, (2014), Macro-segregation characteristics in semi-solid forging of a high strength Al-4.8 Si-0.7 Mg alloy, Materials transactions 55, no. 11.
- [24] Kang, B. Keun, Il Sohn, (2019), Effects of Si Content and Forging Pressure on the Microstructural and Mechanical Characteristics in Semi-solid Forging of Al-Si-Mg Alloys, Metallurgical and Materials Transactions A 50,
- [25] O. Granath, (2007), in: Institutionen för material- och tillverkningsteknik, Chalmers tekniska högskola.
- [26] O. Granath, M. Wessén, H. Cao, (2008), International Journal of Cast Metals Research, 21,349-356.
- [27] M. Bladh, M. Wessén, A.K. Dahle, (2010), Transactions of Nonferrous Metals Society of China, 20, 1749-1755
- [28] H. Cao, M. Wessén, O. Granath, , (2012) International Journal of Cast Metals Research, 23 (2010) 158-163.
- [29] M. Wessén, in: Aluminium Scandinavia, No. 1, pp. 16-17.
- [30] Choi, H.; Konishi, H.; Li, X., (2012), Al2O3 nanoparticles induced simultaneous refinement and modification of primary and eutectic Si particles in hypereutectic Al–20Si alloy. Mater. Sci. Eng. A, 541, 159–165.
- [31] Liu, Zhiyong, Weimin Mao, Tan Wan, Guotao Cui, and Weipan Wang., (2021), Study on semi-solid A380 aluminum alloy slurry prepared by water-cooling serpentine channel and its rheo-diecasting, Metals and Materials International 27, 2067-2077.